Molecular Therapy
Nucleic Acids
Original Article

Supplemental Treatment for Huntington's Disease with *miR-132* that Is Deficient in Huntington's Disease Brain

Masashi Fukuoka,[1,7] Masaki Takahashi,[1,2,7] Hiromi Fujita,[3] Tomoko Chiyo,[4] H. Akiko Popiel,[3] Shoko Watanabe,[5] Hirokazu Furuya,[6,8] Miho Murata,[5] Keiji Wada,[3] Takashi Okada,[4,9] Yoshitaka Nagai,[3,10] and Hirohiko Hohjoh[1]

[1]Department of Molecular Pharmacology, National Institute of Neuroscience, NCNP, Tokyo, Japan; [2]Division of RNA Medical Science, The Institute of Medical Science, The University of Tokyo, Tokyo, Japan; [3]Department of Degenerative Neurological Diseases, National Institute of Neuroscience, NCNP, Tokyo, Japan; [4]Department of Molecular Therapy, National Institute of Neuroscience, NCNP, Tokyo, Japan; [5]National Center Hospital, NCNP, Tokyo, Japan; [6]Oomuta Hospital, Fukuoka, Japan

Huntington's disease (HD) is an intractable neurodegenerative disorder caused by mutant Huntingtin (HTT) proteins that adversely affect various biomolecules and genes. MicroRNAs (miRNAs), which are functional small non-coding RNAs, are also affected by mutant HTT proteins. Here, we show amelioration in motor function and lifespan of HD-model mice, R6/2 mice, by supplying *miR-132* to HD brains using a recombinant adeno-associated virus (rAAV) miRNA expression system. *miR-132* is an miRNA related to neuronal maturation and function, but the level of *miR-132* in the brain of R6/2 mice was significantly lower than that of wild-type mice. Our *miR-132* supplemental treatment, i.e., supplying *miR-132* to the brain, produced symptomatic improvement or retarded disease progression in R6/2 mice; interestingly, it had little effect on disease-causing mutant *HTT* mRNA expression and its products. Therefore, the findings suggest that there may be a therapeutic way to treat HD without inhibiting and/or repairing disease-causing *HTT* genes and gene products. Although *miR-132* supplement may not be a definitive treatment for HD, it may become a therapeutic method for relieving HD symptoms and delaying HD progression.

INTRODUCTION

Huntington's disease (HD; OMIM #143100) is a dominantly inherited neurodegenerative disorder characterized by chorea movement, muscular incoordination, cognitive decline, and psychiatric problems.[1,2] The responsible gene for HD is the *Huntingtin* (*HTT*) gene on chromosome 4p16.3, and aberrantly expanded CAG repeats (translated into polyglutamine tracts) in exon 1 are closely related to the onset and severity of HD;[1,2] such abnormal expansion of the CAG repeat results in unusual aggregation of the HTT protein, which is harmful to neurons in the brain. Currently, there is no definitive treatment for HD, and many efforts have been made to develop better treatments for HD.

MicroRNAs (miRNAs) are 21- to 23-nt-long small noncoding RNAs, which are processed from longer transcripts (primary miRNAs) forming a hairpin structure by digestion with a microprocessor complex containing Drosha and DGCR8 in the nucleus and Dicer in the cytoplasm.[3] After processing, miRNAs are incorporated into the RNA-induced silencing complex (RISC) and function as mediators in gene silencing,[3] which targets mRNAs partially or nearly complementary to the miRNAs. miRNAs play important roles in gene regulation through the gene silencing.

Thousands of miRNA genes have been found in animals and plants (see the microRNA database [miRBase]: http://www.mirbase.org/index.shtml). Expression profiles of miRNAs have been examined, and tissue- and stage-specific expression of miRNAs and disease-associated expression of miRNAs have been detected.[4–10] Thus, miRNAs may become useful biomarkers and may provide us with clues to help better disease treatment.[9–11] Regarding miRNA expression in the brain, a major change in the expression of miRNAs occurs during the first month of mouse life,[12] which corresponds to the stage of rapid brain development. Such controlled expression of miRNAs presumably contributes to normal brain formation and maturation, and abnormal expression of miRNAs due to diseases may cause harmful effects on brain formation.

Disease-causing mutant HTT proteins adversely affect biomolecules such as proteins, mRNAs, and miRNAs in the HD brain. In this study, we examined miRNA expression in the brain of R6/2 (HD-model) mice and wild-type mice, and found that *miR-132* was markedly decreased in HD mice relative to wild-type mice. Previous studies

Received 31 July 2017; accepted 18 January 2018;
https://doi.org/10.1016/j.omtn.2018.01.007.

[7]These authors contributed equally to this work.

[8]Present address: Kochi Medical School, Kochi University, Kochi, Japan

[9]Present address: Department of Biochemistry and Molecular Biology, Nippon Medical School, Tokyo, Japan

[10]Present address: Department of Neurotherapeutics, Osaka University Graduate School of Medicine, Suita, Japan

Correspondence: Hirohiko Hohjoh, PhD, Department of Molecular Pharmacology, National Institute of Neuroscience, NCNP 4-1-1 Ogawahigashi, Kodaira, Tokyo 187-8502, Japan.
E-mail: hohjohh@ncnp.go.jp

Table 1. Difference in the Expression of miRNAs between R6/2 and Wild-Type Mice

	Name[a]	Signal Intensity[b] R6/2	WT	Fold Changes
1	mmu-miR-132-3p	406.7	1238.9	0.33
2	mmu-miR-342-3p	132.2	365.6	0.36
3	mmu-miR-212-5p	64.0	167.8	0.38
4	mmu-miR-132-5p	259.5	643.6	0.40
5	mmu-miR-7646-3p	4.6	10.0	0.46
6	mmu-miR-212-3p	175.0	374.3	0.47
7	mmu-miR-26a-1-3p	3.7	6.6	0.56
8	mmu-miR-7213-3p	7.6	13.5	0.56
9	mmu-miR-299a-5p	48.5	84.9	0.57
10	mmu-miR-128-3p	4,682.7	8,038.4	0.58
11	mmu-miR-182-3p	7.6	12.8	0.60
12	mmu-miR-34a-5p	278.0	464.7	0.60
13	mmu-miR-184-3p	12.2	19.7	0.62
14	mmu-miR-6946-3p	5.3	8.7	0.62
15	mmu-miR-465b-5p	5.4	8.5	0.63
16	mmu-miR-153-3p	1,119.1	1,752.8	0.64
17	mmu-miR-144-5p	4.0	6.1	0.65
18	mmu-miR-205-5p	6.5	10.0	0.65
19	mmu-miR-187-3p	318.3	487.9	0.65
20	mmu-miR-708-5p	245.1	369.8	0.66

10-week-old same littermate mice (male) were examined. WT, wild-type.
[a]The top 20 miRNAs that markedly decreased in R6/2 mouse are indicated.
[b]Hybridization signal intensities obtained from DNA chip analysis are indicated.

suggested that *miR-132* is a key miRNA involved in neuronal maturation and function.[13–15] Based on the findings, we conducted a therapeutic trial to reduce the shortage of *miR-132* in the HD brains by supplying *miR-132* using an AAV miRNA expression system in this study, and we showed symptomatic improvement in motor function and lifespan of treated HD mice without suppressing disease-causing mutant HTTs.

RESULTS

miR-132 Deficiency in the Brain of HD Mice

We investigated miRNA expression in the striatum, a major HD focus, of R6/2 (HD-model) and wild-type mice by means of DNA chip technology, and found that *miR-132* and its adjacent, analogous *miR-212*[13,16] were markedly decreased in HD mice relative to wild-type mice (Table 1); note that *miR-212* was considerably less than *miR-132* (Figure S1). The results were confirmed by northern blotting as well (Figure 1A), and the findings were consistent with previous studies:[17,18] another HD model of YAC128 mice expressing full-length mutant *HTT* mRNAs showed a decrease in *miR-132* in the brain,[17] and more noteworthy, Johnson et al.[18] indicated that *miR-132* levels were decreased in post-mortem brains of HD patients. Thus, there may be some association between *miR-132* and HD.

The expression of *miR-132* was examined in detail by means of qRT-PCR, because a major change in miRNA expression occurs in the mouse brain during the first month after birth.[12] The resultant expression profiles exhibited that the post-natal *miR-132* of HD mice was expressed in the same manner as wild-type mice, but soon reached a plateau at lower levels than wild-type mice (Figure 1B). Consequently, a significant decrease in *miR-132* levels occurred in HD mouse brains.

In addition to the findings, we investigated *miR-132* levels in various tissues of HD and wild-type mice (Figure S2), and also in human HD lymphoblastoid cell lines (Figure S3). Although the *miR-132* expression levels of the examined tissues were significantly lower than that of the brain, the decreasing trend of the *miR-132* level in HD as compared with normal controls appeared to be kept in the tissues examined except for the liver and kidney.

Decrease in *miR-132* Associated with Ago2

To see whether *miR-132* deficiency affected *miR-132*-involved gene silencing, we investigated *miR-132* associated with Argonaute 2 (Ago2), which is an essential protein having endonuclease activity according to miRNA in the RISC.[3] First we examined striatal Ago2 in HD and wild-type mice by western blotting. As a result, Ago2 had little difference between the two mice (Figure 2A), suggesting that there might be no difference in the ability of Ago2 itself between HD and wild-type mice. We then investigated *miR-132* associated with Ago2. Immunoprecipitation with anti-Ago2 antibodies followed by qRT-PCR to detect miRNAs in immunoprecipitates was carried out (Figures 2B–2D). *miR-132*, *-125a,b*, and *-128* were examined, and in this assay, *miR-125b* was used as an internal control because *miR-125b* levels were nearly similar between HD and wild-type mice (Figures 2C and 2D). The results indicated that the level of *miR-132* associated with Ago2 in HD mice was markedly lower than that in wild-type mice (Figure 2D). In addition, *miR-125a* and *-128* associated with Ago2 as well decreased in HD mice relative to wild-type mice (Figure 2D). Therefore, a decrease in *miR-132*, *-125a*, and *-128* may confer a decrease in their gene silencing activities.

Expression of the Target Genes of *miR-132*

We examined the following *miR-132* target genes: *Methyl-CpG binding protein 2* (*MeCP2*),[19] *Rho GTPase activating protein 32* (*p250GAP*),[20–22] *Polypyrimidine tract binding protein 2* (*Ptbp2*),[23] and *Regulatory factor X4* (*Rfx4*).[24] The protein levels of striatal MeCP2, p250GAP, Ptbp2, and Rfx4 were examined by western blotting. Compared with wild-type mice, MeCP2 and Ptbp2 of HD mice increased, whereas p250GAP decreased, and Rfx4 appeared to slightly decrease in HD mice (Figure 3A). The mRNA levels of *Ptbp2* and *Rfx4* showed little difference between HD and wild-type mice, whereas MeCP2 slightly increased in HD mice, and *p250GAP* decreased (Figure 3B). Based on the principle of miRNA-mediated gene silencing, a decrease in miRNAs should result in an increase in their target gene products. Accordingly, *MeCP2* and *Ptbp2* might be candidate genes that are affected by the shortage of *miR-132* in the brain. The protein

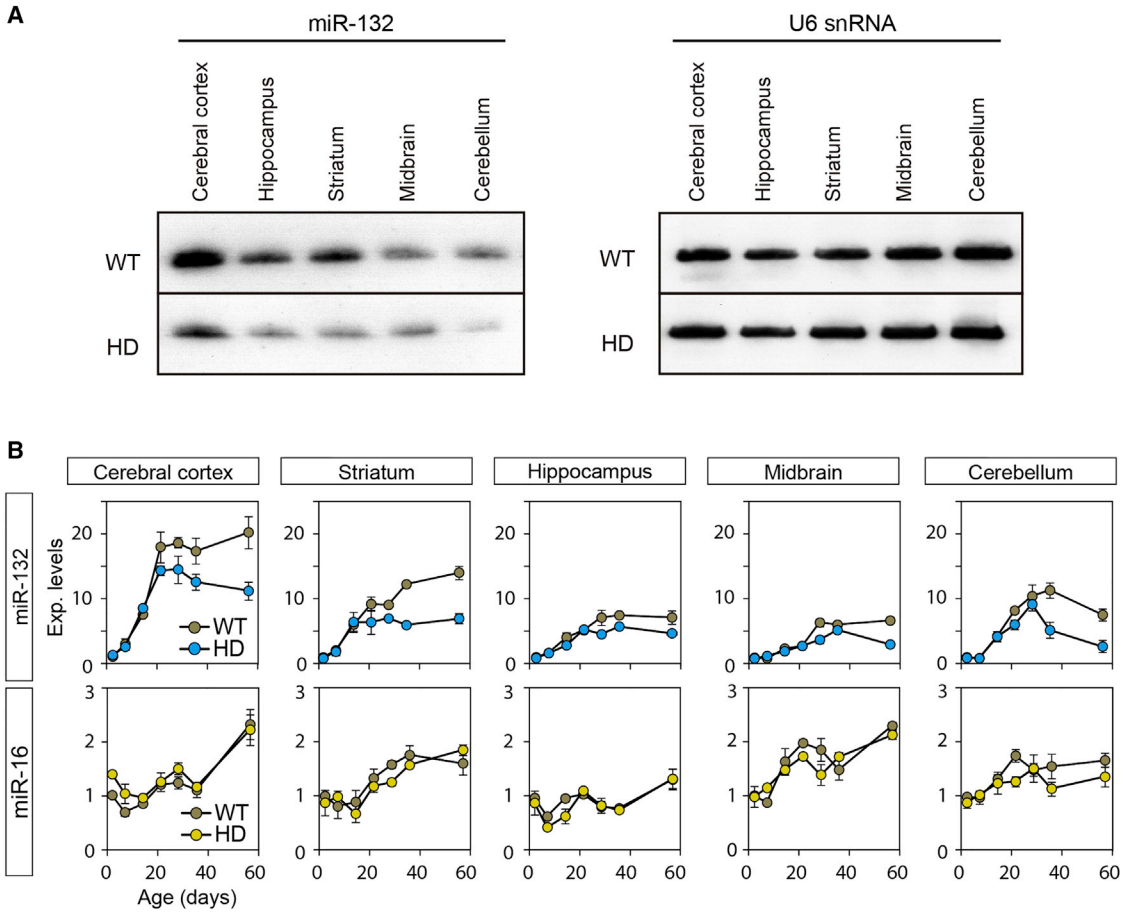

Figure 1. Expression Profiles of miRNAs in HD and Wild-Type Mouse Brains

(A) Northern blot analysis. Small RNAs were extracted from five brain subregions of R6/2 (HD) and wild-type (WT) mice aged 9 weeks, and were subjected to Northern blot analysis using 5′-DIG-labeled miRCURY LNA miRNA detection probes against *miR-132* and *U6 snoRNA* as a control. (B) qRT-PCR analyses of *miR-132* and *miR-16*. Five brain subregions indicated were collected from HD and WT mice at post-natal days 2, 7, 14, 21, 28, 35, and 56. The expression levels of *miR-132*, *-16*, and *U6 snoRNA* were examined and analyzed by a delta Ct (threshold cycle) method using the level of *U6 snoRNA* as a control. The normalized miRNA levels were further normalized by the level obtained in WT mice at post-natal day 2 as 1. Data are shown as mean ± SEM (n = 4 individual mice).

level of p250GAP appears to directly reflect its mRNA level, and Rfx4 may be similar as well.

miR-132 Supplement into the Brain of HD Mice

Because previous studies suggested that *miR-132* made an important contribution to neuronal function and maturation,[14,15,21,25] we conducted therapeutic trials to see what would happen to HD mice if *miR-132* were supplied to the HD brains. To compensate for the shortage of *miR-132* in HD brains, we constructed a viral *miR-132*-expression system using recombinant adeno-associated viruses (rAAVs). The constructed *miR-132*-expression viruses (AAV9_miR-132) and negative-control viruses (AAV9_miR-Neg) were introduced into the striatum of ≈3-week-old HD and wild-type mice (Figure 4A); that age was when the marked difference in *miR-132* levels began to appear between the mice (Figure 1B). After virus inoculation, *miR-132* levels were examined and confirmed to return to normal levels in the striatum of AAV9_miR-132-treated HD mice (Figure 4B). Consistently, the level of *miR-132* associated with Ago2 markedly increased in AAV9_miR-132-treated HD and wild-type mice (Figure 4C). An increase in *miR-132* was also detected in the cerebral cortex and the midbrain of the AAV9_miR-132-treated HD mice. This was probably due to the diffusion of AAV9_miR-132 viruses (Figure S4).

MeCP2 and *Ptbp2*, which are candidates of *miR-132* targets (Figure 4D), were examined. As a result, the MeCP2 protein was reduced in AAV9_miR-132-treated mice without a decrease in MeCP2 mRNA levels (Figure S5A), compared with AAV9_miR-Neg-treagted mice. Note that the decrease in MeCP2 was seen in both AAV9_miR-132-treated wild-type and HD mice. In contrast, the *Ptbp2* gene products appeared to remain unchanged between AAV9_miR-132-treated and AAV9_miR-Neg-treated mice (Figure 4D; Figure S5B). Thus, the findings suggest that *MeCP2* may be a target gene of *miR-132* in the brain.

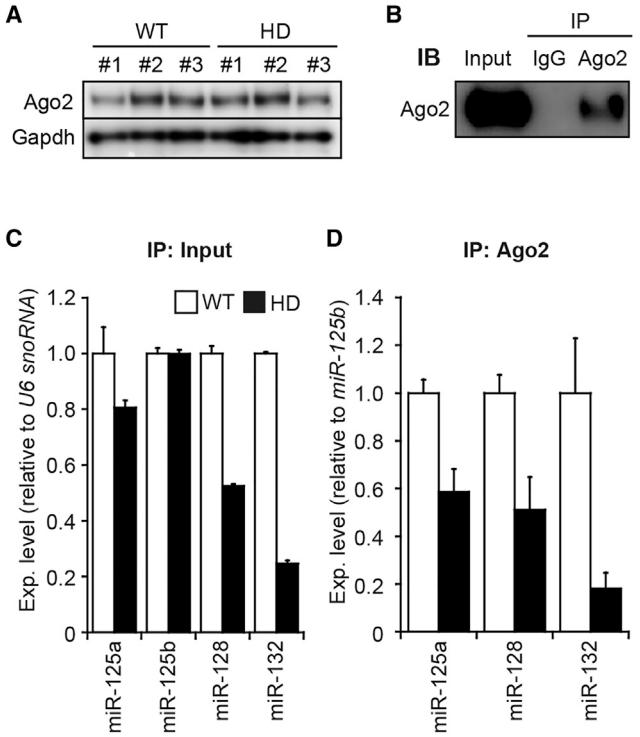

Figure 2. miRNAs Associated with Ago2

(A) Striatal Ago2. Striatal tissues were isolated from R6/2 (HD) and wild-type (WT) mice aged 8 weeks and examined by western blotting using anti-Ago2 antibodies and Gapdh antibodies as an internal control. Numbers (#1–3) in WT and HD represent individual mice examined. (B) Western blot analysis of immunoprecipitates. Immunoprecipitates by indicated antibodies (IP) from whole brain extracts prepared from 4-month-old wild-type mice were examined by western blotting using anti-Ago2 antibodies (IB). Whole brain extracts as a source of immunoprecipitation (Input) were also examined. (C) miRNA expression in the striatum of 12-week-old HD and WT mice. Indicated miRNAs were examined by qRT-PCR as in Figure 1B. The levels of the miRNAs were normalized to the level of *U6 snoRNA* as a control and further normalized by the levels obtained in WT mice as 1. Data are shown as mean ± SEM (n = 3 measurements). (D) miRNAs associated with Ago2. Immunoprecipitation with anti-Ago2 antibodies from the same striatal samples as in (C) was performed, and miRNAs coimmunoprecipitated with the antibodies were examined by qRT-PCR. The levels of the miRNAs were normalized to the *miR-125b* levels; this is because *U6 snoRNA* hardly associated with Ago2 and because the *miR-125b* levels were similar between HD and WT mice (as shown in C). The normalized miRNA levels were further normalized by the level obtained in WT mice as 1. Data are shown as mean ± SEM (n = 3 measurements). IgG, a control IgG.

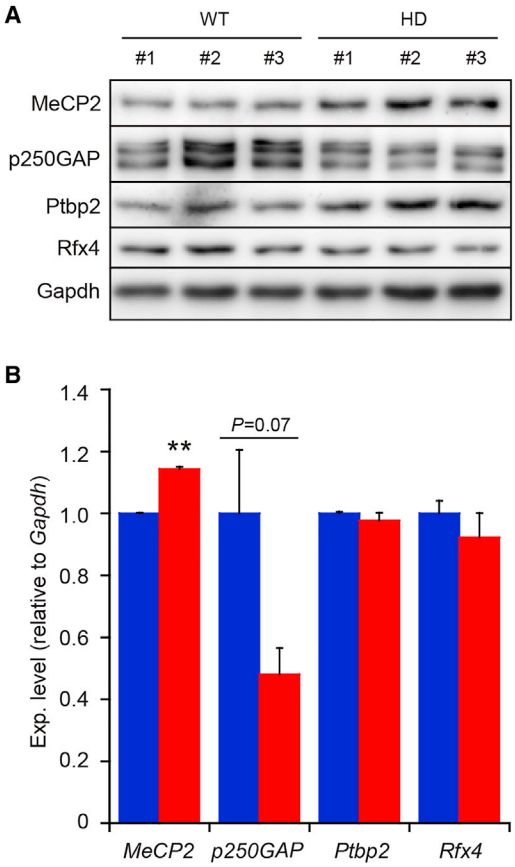

Figure 3. Expression of *miR-132* Target Gene Products

The proteins (A) and mRNA levels (B) of *miR-132* target genes in the striatum of R6/2 (HD) and wild-type (WT) mice at the age of 8 weeks were examined by western blotting and qRT-PCR, respectively. In western blotting, numbers (#1–3) in WT and HD represent individual mice examined. Gapdh was examined as an internal control. In mRNA analysis, the mRNA levels of the target genes were normalized to the level of *Gapdh* as an internal control and further normalized to the level obtained from WT mice as 1 (blue bars). Data are shown as mean ± SEM (n = 3 individual mice, **$p < 0.01$ by Student's t test).

Symptomatic Improvement of Motor Function and Lifespan in AAV9_miR-132-Treated HD Mice

Because R6/2 mice are well known as a fulminant HD-model animal suffering from severe motor deficits and rapidly declining locomotor activity,[26,27] we investigated the behavior and longevity of AAV9_miR-132-treated HD mice and also AAV9_miR-Neg-treated HD mice (as controls). Interestingly enough, *miR-132* supplementation produced symptomatic improvement, i.e., rotarod and open-field test showed a definite amelioration in AAV9_miR-132-treated HD mice (Figure 5A; Figure S6). Moreover, AAV9_miR-132-treated HD mice showed a significant life prolongation relative to AAV9_miR-Neg-treated HD mice (Figure 5B) and also exhibited a slight increase in body weight (Figure S6D). Therefore, the findings strongly suggested that *miR-132* recovery was effective in improving motor function of HD mice and prolonging their life, or effective in slow disease progression in HD mice.

Regarding AAV9_miR-132-treated wild-type mice, *miR-132* exceeding normal levels was expressed in the brain (Figures 4B and 4C), but there was little or no difference in behavior and longevity between AAV9_miR-132-treated and AAV9_miR-Neg-treated wild-type mice (Figure 5). In addition, no significant change had been observed afterward. Thus, it is possible that a deficiency of *miR-132* may have a major impact on the life of the mouse, but a surplus of *miR-132* may not have.

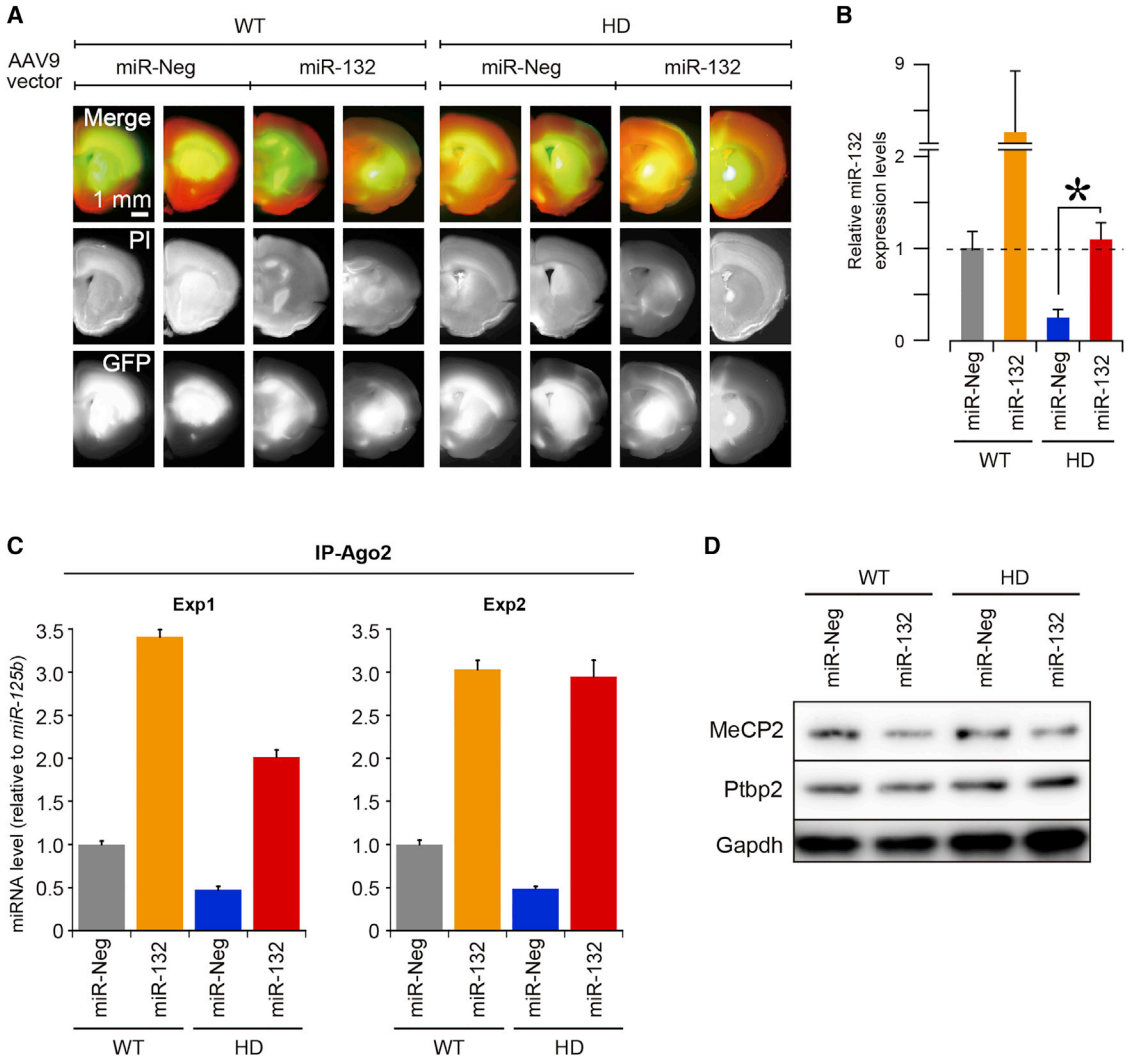

Figure 4. Administration of AAV9_miR-132 and AAV9_miR-Neg Viruses to HD and WT Mice

(A) Histological examination. AAV9_miR-132 and AAV9_miR-Neg as a control were injected into both sides of the striatum of HD and wild-type (WT) mice aged 3 weeks. AAV9_miR-Neg expresses a short hairpin RNA just as a regular pre-miRNA, but is predicted not to target any known gene. Four weeks after injection, the brains were isolated, fixed with 4% PFA at 4°C overnight, and subjected to brain slicing (coronal section, approximately 1 mm thick). The brain slices were stained with propidium iodide, and the signals of propidium iodide (red) and the GFP reporter protein (green) derived from the AAV9 vectors were examined by a fluorescence stereo microscope. Two individual mice in each treated group were examined. (B) The expression levels of *miR-132* in the striatum of the treated HD and WT mice at the age of 7 weeks (4 weeks after administration) were examined by qRT-PCR as in Figure 1B. The data were normalized to the level obtained from WT mice treated with AAV9_miR-Neg as 1 (n = 4 individual mice; *$p < 0.05$ by Tukey-Kramer test). Data are shown as mean ± SEM. (C) *miR-132* associated with Ago2. HD and WT mice treated with AAV9_miR-132 and AAV9_miR-Neg were examined as in (B). Immunoprecipitation (IP) with anti-Ago2 antibodies and miRNA analysis were performed as in Figure 2. The *miR-132* levels normalized to the *miR-125b* levels were further normalized to the levels obtained from AAV9_miR-Neg-treated WT mice as 1 (gray bars). The experiment was duplicated (Exp 1 and 2). Data are shown as mean ± SEM (n = 3 measurements). (D) MeCP2 and Ptbp2 expression. The MeCP2 and Ptbp2 proteins in the striatum of HD and WT mice treated with AAV9_miR-132 (miR-132) and AAV9_miR-Neg (miR-Neg) were examined by western blotting as in Figure 3. Gapdh was examined as an internal control.

From the findings, we raised the working hypothesis that *miR-132* supplement might suppress the expression of disease-causing mutant *HTTs* and be capable of eliminating harmful mutant HTTs from the HD brain. To address the hypothesis, we examined mutant *HTT* expression by RT-semiquantitative PCR. As a result, the mutant *HTT* level hardly changed between AAV9_miR-132-treated and AAV9_miR-Neg-treated HD mice (Figure 6). We further performed an immunohistochemical analysis for detection of mutant HTT inclusion bodies that are characteristic of HD.[28] The results indicated that there was no significant difference in formation of inclusion bodies between AAV9_miR-132-treated and AAV9_miR-Neg-treated HD mice (Figure 7A). Western blot analysis of the striatum

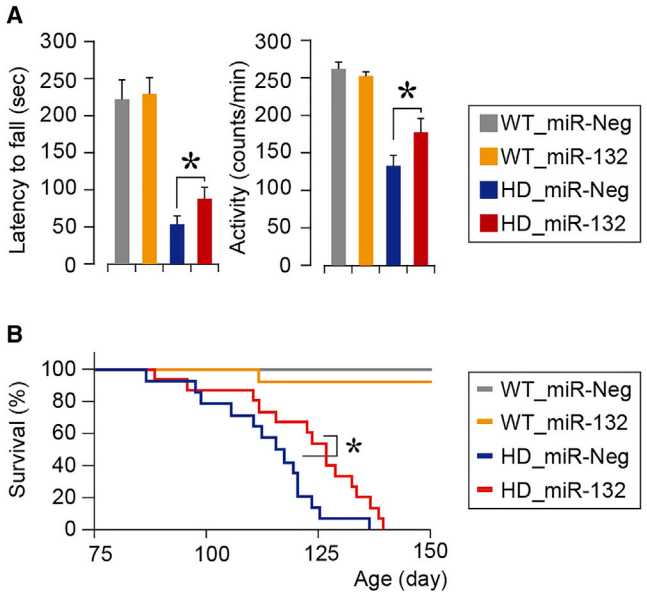

Figure 5. Effects of *miR-132* Supplement on HD Mice

(A) Motor function tests. AAV9_miR-132- and AAV9_miR-Neg-treated mice at the age of 11 weeks (8 weeks after administration) were examined by rotarod test (left panel) and open field activity test (right panel) (*$p < 0.05$ by Tukey-Kramer test). The HD mice injected with AAV9_miR-132 and AAV9_miR-Neg are indicated in red and blue, respectively, and the wild-type (WT) mice injected with AAV9_miR-132 and AAV9_miR-Neg are indicated in yellow and gray, respectively. Data are shown as mean ± SEM. Details of the tests are in the Materials and Methods. (B) Survival curve. The number of mice examined was as follows: 14 HD mice injected with AAV9_miR-132 (in red), 13 HD mice injected with AAV9_miR-Neg (in blue), 14 WT mice injected with AAV9_miR-132 (in yellow), and 16 WT mice injected with AAV9_miR-Neg (in gray). Kaplan-Meier survival analysis was performed (*$p < 0.05$ by log rank test).

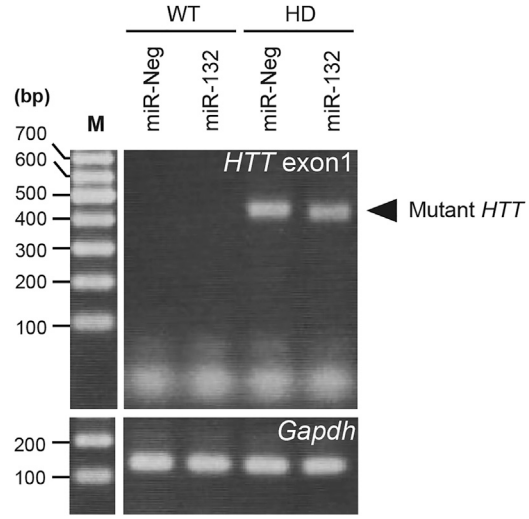

Figure 6. Mutant *HTT* Expression

Total RNAs used in Figure 4B were examined by RT-semiquantitative PCR to see mutant *HTT* expression. PCR products were analyzed by agarose gel electrophoresis followed by ethidium bromide staining. *Gapdh* was also examined as an internal control.

also exhibited a compatible result: there was little difference in mutant HTT between AAV9_miR-132-treated and AAV9_miR-Neg-treated HD mice (Figure S7). In addition, consistent results were obtained from *in vitro* experiments as well using primary neurons co-expressed with exogenous mutant *HTT* and *miR-132* (Figure 7B). Consequently, these unexpected findings suggested that *miR-132* supplementation had little effect on the expression of mutant HTTs and their inclusion body formation in HD mice supplemented with *miR-132*.

DISCUSSION

Supplemental miRNA Therapy

Inhibition of disease-causing genes or elimination of mutant gene products is a straightforward and ideal approach for the treatment of intractable diseases caused by dominant-negative disease-causing genes such as mutant *HTT* genes in HD. Specific inhibition of disease-causing genes carrying nucleotide variations may be feasible by specific silencing such as disease-causing allele-specific RNAi;[29–32] however, RNAi may be difficult to eliminate disease-causing gene products thoroughly from patients' cells. For fighting against intractable diseases, it is necessary to develop other treatment approaches based on mechanisms of action different from conventional approaches, even if such approaches had the only effect of symptomatic relief. Our current study offers the suggestion that miRNAs may open up a new way of treatment for HD, i.e., miRNA supplemental therapy.

In the current study, we focused on *miR-132* that markedly decreased in the brain of HD mice (Table 1; Figure 1). Our therapeutical trial using *miR-132*-expression AAVs showed that *miR-132* supplement for reducing the deficiency of *miR-132* in the HD brains conferred amelioration in motor function and lifespan of HD mice (Figure 5). In addition, it is noteworthy that *miR-132* supplement hardly affected disease-causing *HTT* genes and their gene products (Figures 6 and 7; Figure S7); i.e., such a symptomatic improvement was gained without suppressing and/or eliminating harmful mutant HTTs. The findings provided us with a new insight into the treatment strategy for HD; that is, there may be a therapeutic approach to HD without inhibiting disease-causing mutant HTTs.

On a relevant note, Benraiss et al.[33] recently demonstrated that a striatal transplantation of normal human glia into the brain of R6/2 mice resulted in amelioration in the HD phenotype without influencing mutant HTTs, and another recent study in which 589,306 human genomes were analyzed indicated that there were healthy individuals possessing highly penetrant, deleterious disease-causing alleles.[34] These findings surprised us and suggested that there may be a mechanism(s) by which deleterious effects caused by harmful mutations would be alleviated without wiping out the mutations. Therefore, these studies and also our study suggested that there might be a therapeutic way to treat intractable diseases without inhibiting and/or repairing disease-causing genes and gene products.

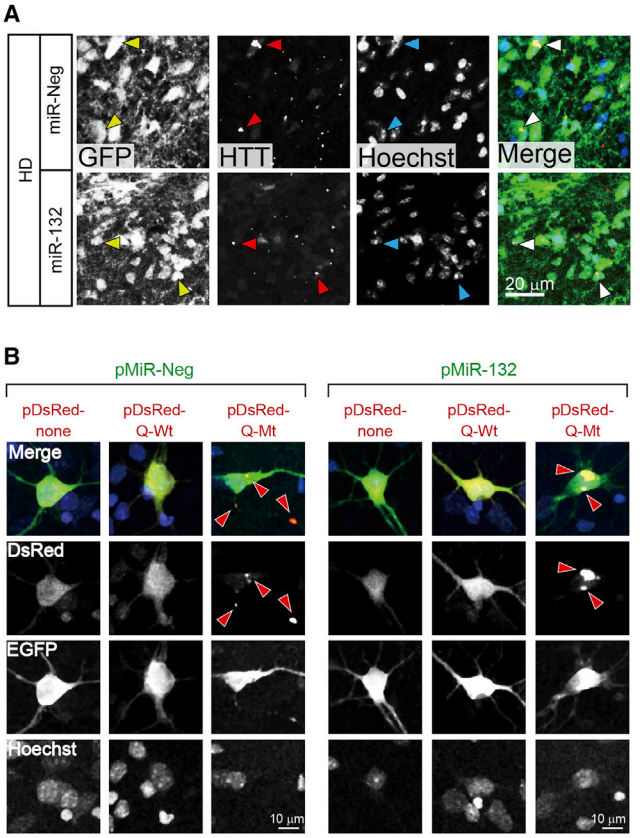

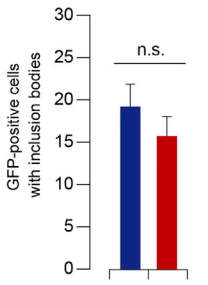

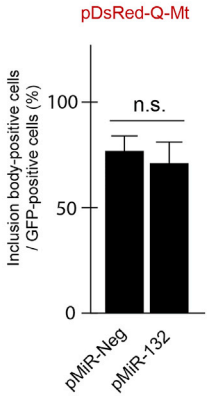

Figure 7. Inclusion Body Formation under *miR-132* Supplementation

(A) Immunohistological analysis. HD mice treated with AAV9_miR-132 (red bar) and AAV9_miR-Neg (blue bar) were examined 4 weeks after AAV9 administration as in Figure 4A. Sagittal brain sections were prepared and subjected to fluorescent immunostaining with anti-GFP and anti-HTT antibodies and counterstaining with Hoechst 33342. Arrowheads indicate inclusion bodies observed in GFP-positive cells (AAV9-infected cells). The GFP-positive cells containing inclusion bodies were counted in three different fields of view (a field of view = 247 μm × 247 μm) per individual mice. Data are shown as mean ± SEM (n = 3 mice) in the bar graph. n.s., no significant difference. (B) Inclusion bodies in neuronal cells supplemented with *miR-132*. Cultured neurons were transfected with pMiR-132 or pMiR-Neg, both of which encode the *GFP* reporter gene, together with pDsRed-Q-Wt (normal HTT) or pDsRed-Q-Mt (mutant HTT). Two days after transfection, the cells were fixed and stained with Hoechst 33342. Inclusion bodies (indicated by arrowheads) were detected only in cells transfected with pDsRed-Q-Mt. The percentage of inclusion body-positive cells in GFP-positive cells was examined. Data are shown as mean ± SEM (n = 13 and 16 GFP-positive cells in pMiR-Neg and pMiR-132 transfection, respectively). n.s., no statistical difference by Student's t test.

This new strategy may further expand the versatility of the treatment approach to other diseases. Downregulation of *miR-132*/*miR-212* was also detected in the brain of patients with Alzheimer's disease[35–37] and schizophrenia,[38] other than HD.[18] Therefore, *miR-132* supplement might be available and effective for the cure of such diseases in which *miR-132* is deficient, whatever the causative disease genes. In conclusion, although *miR-132* supplementation may not be a definitive therapy for HD, it may become an adjunctive therapy for HD, which may help to delay the onset of disease and the progression of disease.

The current study has left a challenge; i.e., the mechanism of improvement by suppling *miR-132* to the HD brain remains unknown. The AAV9_miR-132 virus appears to supply enough *miR-132* to compensate for *miR-132* deficiency in the HD brain (Figure 4), and the supplied *miR-132* can associate with Ago2 (Figure 4C) and probably function properly. As a result, symptomatic improvement would be brought to HD mice (Figure 5). *miR-132*-mediated gene silencing would recover after AAV9_miR-132 virus inoculation and *MeCP2* as a target of *miR-132* appeared to undergo translation inhibition. McFarland et al.[39] indicated that the association of Htt with MeCP2 increased in knock-in *Hdh* mice (another HD model), suggesting that abnormal interaction between Htt and MeCP2 may cause transcriptional dysregulation. Based on the previous study, an increase in MeCP2 in R6/2 mice might promote abnormal interaction between mutant HTT and MeCP2; thus, the decrease in MeCP2 by *miR-132* supplement might reduce the aberrant interaction. As for *miR-132* targets examined other than MeCP2, curiously, the relationship with *miR-132* appeared to be inconsistent with the mechanism of miRNA-mediated gene silencing (Figure 3). In this regard, mutant HTTs might have some effect on certain *miR-132* target mRNAs in HD mice. In any case, there is little information on the mechanism of action for amelioration of HD symptoms when *miR-132* is supplied to *miR-132*-deficient HD mice. As a clue to the solution, authentic target genes, like *MeCP2*, that respond to *miR-132* in HD mice may be the key molecules to understand the mechanism of action. Because *miR-132* is involved in various elements related to neurons such as neuronal structure and function, it is possible that there are *miR-132* target genes that have not been found yet. Among such target genes, there may be major targets contributing to amelioration in HD mice under *miR-132* supplementation. To elucidate the mechanism of action for ameliorating symptoms of HD by *miR-132* supplement, more extensive studies including the identification of major target genes are needed and remain to be carried out.

MATERIALS AND METHODS

Animals

R6/2 mice, which carry a mutant human *HTT* exon1 containing abnormally expanded CAG repeats,[26] were purchased from Jackson Laboratory (Bar Harbor, ME, USA) and maintained as described

previously.[26,40] Identification of the mutant mice was performed by genotyping using PCR as described previously.[26,40] Our sequence analysis of the PCR products indicated that the mutant mice maintained approximately 124 CAG repeats in the *HTT* exon1. Mice were housed, fed, and maintained in the laboratory animal facility according to the National Institute of Neuroscience animal care guidelines. All the animal experiments were performed in strict accordance with the recommendations in the Guide for the Care and Use of Laboratory Animals of the National Institutes of Neuroscience. The protocols were approved by the Committee on the Ethics of Animal Experiments of the National Institutes of Neuroscience (Permit Number: 2015003).

DNA Oligonucleotides

DNA oligonucleotides used in this study were synthesized by and purchased from Sigma-Aldrich (St. Louis, MO, USA).

miRNA Expression Profile Analysis

Total RNAs were extracted from the striatum of 10-week-old R6/2 mouse (male) and littermate wild-type mouse (male). RNAs were subjected to a comprehensive miRNA expression analysis using 3D-Gene Mouse miRNA (Ver.21) chips according to the protocols supplied by TORAY Industries (Tokyo, Japan). Hybridization signals were examined by a 3D-Gene Scanner 3000 followed by quantifying with Extraction according to the manufacturer's instructions (TORAY). Obtained miRNA expression profile data were deposited to the GEO in NCBI.

Northern Blot

Small RNA fractions were extracted from brain subregions by a *mir*Vana miRNA Isolation Kit (Thermo Fisher Scientific) according to the manufacturer's instructions. Aliquots of small RNA ($\approx$0.48 μg/each sample) were electrophoretically separated in 8 M urea denatured (15%) polyacrylamide gels and transferred onto positively charged nylon membranes. The membranes were hybridized with 5′-DIG-labeled miRCURY LNA miRNA detection probes (EXIQON, Velbaek, Denmark) at 65°C for 15 hr. After washing the membranes, the hybridized probes were detected by an alkaline phosphatase-conjugated anti-DIG antibody (Roche, Basel, Switzerland) and a chemiluminescent detection system.

RT-PCR

Total RNAs were extracted from brain subregions and cultured cells using a TRI REAGENT (Sigma-Aldrich) according to the manufacturer's instructions and subjected to qRT-PCR. Real-time PCR was performed using an AB7300 Real Time PCR System (Thermo Fisher Scientific, Waltham, MA, USA) with a TaqMan Universal PCR Master Mix together with TaqMan MicroRNA Assays (Thermo Fisher Scientific) according to the manufacturer's instructions. TaqMan MicroRNA Assays used are as follows (manufacturer's assay IDs are indicated in parentheses): *hsa-miR-16* (000391), *hsa-miR-125a* (000448), *hsa-miR-125b* (000449), *hsa-miR-128a* (002216), *hsa-miR-132* (000457), *hsa-miR-212* (000515), and *U6 snoRNA* (001973).

To see the expression of mutant *HTT* in R6/2 brains, total RNA prepared from the brain was subjected to RT with oligo (dT) primers (Promega, Fitchburg, WI, USA) followed by semiquantitative PCR using a GeneAmp PCR system 9700 (Thermo Fisher Scientific). The resultant PCR products were examined by agarose gel electrophoresis followed by ethidium bromide staining. The sequences of the PCR primers used are indicated in Table S1. *Gapdh* was examined as an internal control, and its PCR primers were purchased from TAKARA BIO (primer set ID: MA050371; Otsu, Shiga, Japan).

To examine the expression of *miR-132* targets, total RNA prepared from the brain was subjected to RT with oligo (dT) primers (Promega) followed by real-time PCR. Real-time PCR was carried out using an AB7300 Real Time PCR System (Thermo Fisher Scientific) with a FastStart Universal SYBR Green Master (Roche). PCR primers (TAKARA BIO) used are as follows (primer set IDs are indicated in parentheses): *MeCP2* (MA079473), *p250GAP(Arhgap32)* (MA170683), *Ptbp2* (MA168870), *Rfx4* (MA110752), and *Gapdh* (MA050371).

Immunoprecipitation

Whole brain or striatal tissue was homogenized in 1 mL of ice-cold lysis buffer (10 mM HEPES [pH 7.4], 200 mM NaCl, 30 mM EDTA, 0.5% Triton X-100, 0.4 U/μL RNasin Plus RNase inhibitor [Promega], 1× Protease/Phosphatase inhibitor Cocktail [CST, Danvers, MA, USA]). Lysate was centrifuged at 3,000 × *g* for 10 min at 4°C, and the supernatant was transferred into a new 1.5-mL tube. The NaCl concentration in the supernatant was adjusted to 400 mM with 5 M NaCl; then a part of the supernatant was taken and stored as a crude lysate sample. The rest was centrifuged at 70,000 × *g* for 20 min at 4°C, and the supernatant was mixed with yeast tRNAs (100 μg/mL final concentration) (Sigma-Aldrich) and pretreated with 40 μL of protein A-Sepharose 4B slurry (Sigma-Aldrich) for 30 min at 4°C. After centrifugation at 12,000 × *g* for 2 min at 4°C, a part of the supernatant was taken and stored as an immunoprecipitation (IP) input sample, and the remaining supernatant was divided equally. The divided samples were added with anti-AGO2 IgG (2897S; CST) and a control IgG (3900S; CST), respectively, and gently mixed using a rotator overnight at 4°C. Protein A-Sepharose 4B slurry (20 μL/each) was added to the treated samples and incubated further for 1 hr at 4°C with gently mixing. After incubation, the protein A-Sepharose beads were collected by centrifugation at 12,000 × *g* for 2 min at 4°C, washed four times with 0.4 mL of wash buffer 1 (the lysis buffer containing 0.04 U/μL RNasin Plus RNase inhibitor, 10 μg/mL yeast tRNAs, and 0.1× Protease/Phosphatase inhibitor Cocktail [1:1,000; CST]), and finally washed with 0.5 mL of wash buffer 2 (the wash buffer 1 without yeast tRNAs and RNasin Plus RNase inhibitor). RNAs co-precipitated with the protein A-Sepharose beads were extracted with TRI REAGENT according to the manufacturer's instructions (Sigma-Aldrich). For protein extraction, the beads were treated with 2× sample buffer (125 mM Tris-HCl [pH 6.8], 2% glycerol, 4% SDS, 0.02% bromophenol blue, and 10% beta-mercaptoethanol]) and boiled for 5 min followed by centrifugation at 12,000 × *g* for 2 min at 4°C. The

supernatant was collected and examined by western blotting using an anti-Ago2 antibody (ab32381; Abcam).

Construction of Plasmids and Viruses

Construction of miR-132 Expression Plasmid and Virus

Synthetic oligoDNA duplex that encodes the *miR-132* gene was inserted into pcDNA 6.2-GW/EmGFP-miR expression vector using a BLOCK-iT Pol II miR RNAi Expression Vector Kit with EmGFP (Thermo Fisher Scientific) according to the manufacturer's instructions. The sequences of the *miR-132* oligoDNAs inserted into the vector are indicated in Table S1. The constructed plasmid, named pMiR-132, carries *miR-132* in the 3′ UTR of the *GFP* reporter gene. The pcDNA 6.2-GW/EmGFP-miR-neg control plasmid provided by the manufacturer was used as a negative control and named pMiR-Neg in this study. The pMiR-Neg plasmid encodes a short hairpin RNA just as a regular pre-miRNA, but the hairpin RNA is predicted not to target any known vertebrate gene.

For construction of expression viruses, the *GFP* reporter genes containing *miR-132* and *miR-neg* in pMiR-132 and pMiR-Neg, respectively, were amplified by PCR using a PrimeSTAR HS DNA Polymerase with GC buffer (TAKARA BIO) and PCR primers. The sequences of the PCR primers used are indicated in Table S1. The PCR products were purified by a PCR & Gel purification kit (BEX, Itabashi-ku, Tokyo, Japan) according to the manufacturer's instructions and subjected to ligation with pW-CAG-EGFP-WPRE vector digested with *Eco*RI and *Bam*HI, using an In-Fusion HD Cloning Kit (TAKARA BIO) according to the manufacturer's instructions. The resultant pW-CAG-EGFP-WPRE vectors containing *miR-132* or *miR-Neg* were packed into recombinant adeno-associated viruses based on serotype 9 (rAAV-9) as described previously.[41] The rAAV-9 viruses encoding *miR-132* and *miR-Neg*, named AAV9_miR-132 and AAV9_miR-Neg, respectively, were used in this study.

HTT Expression Plasmids

The pEGFP-Q22 and pEGFP-Q145 plasmids that encode normal (22 CAG repeats) and abnormal (145 CAG repeats) *HTT* exon1 sequences, respectively, were used.[42] In the plasmids, the *HTT* exon1 is fused with the *EGFP* reporter gene. We further constructed pDsRed-Q-Wt and pDsRed-Q-Mt plasmids, which encoded the normal and abnormal *HTT* exon1, respectively. In the plasmids, the *HTT* exon1 is fused with the *DsRed*-monomer gene derived from pDsRed-monomer vector (TAKARA BIO).

Primary Cortical Neuron and Astrocyte Culture

Mouse primary neuronal cells were prepared and cultured. In brief, mouse embryonic day 17 (E17) embryonic cerebral tissue (ICR mouse strain) was isolated, treated with 0.5% trypsin-EDTA solution containing 0.1 mg/mL DNase I (Roche) and 5 mg/mL glucose at 37°C for 20 min, dissociated by pipetting several times, and passed through a 70-μm nylon filter (DB, Franklin Lakes, NJ, USA). The dissociated neuronal cells were seeded on poly-L-lysine (Sigma-Aldrich)-coated culture plates (a cell density of 4×10^3 cells/mm^2) and cultured at 37°C in Neurobasal medium (Thermo Fisher Scientific) supplemented with 1% FBS (Life Technologies), 2% B27 supplement (Thermo Fisher Scientific), 1 mM glutamine (Sigma-Aldrich), and 10 μM 2-mercaptoethanol (Sigma-Aldrich) in a 5% CO_2 humidified chamber. For astrocyte separation, 1-week-cultured cells were trypsinized and then sub-cultured on normal tissue culture plates (cell density of 4×10^3 cells/mm^2) in DMEM (Thermo Fisher Scientific) supplemented with 10% FBS, 110 mg/L sodium pyruvate (Thermo Fisher Scientific), and 1× antibiotics (25 mg/L streptomycin and 50 U/mL penicillin; Wako, Chuo-ku, Osaka, Japan). Cells were grown at 37°C in a 5% CO_2 humidified chamber, and sequential passage of the cells was performed.

Isolation of Lymphocytes from Mice Blood

Whole blood of mice was collected by cardiac puncture using a 26G-needle syringe containing 0.1 mL of 10 mg/mL EDTA. The blood samples were transferred into 15-mL tubes and mixed with 10 mL of RBC lysis buffer (10 mM NH_4HCO_3, 144 mM NH_4Cl). Lymphocytes were collected by centrifugation at 1,600 × *g* for 10 min. Cells were washed four times with RBC lysis buffer and subjected to RNA extraction using a TRI REAGENT (Sigma-Aldrich).

Lymphoblastoid Cell Culture

Epstein-Barr virus-transformed human lymphoblastoid cell lines were cultured at 37°C in RPMI 1640 medium (Sigma-Aldrich) supplemented with 10% FBS (Japan Bio Serum, Fukuyama, Hiroshima, Japan), 110 mg/L sodium pyruvate (Wako), 4,500 mg/L D-glucose (Wako), 100 U/mL penicillin, and 100 μg/mL streptomycin (Thermo Fisher Scientific) in a 5% CO_2 humidified chamber.

Intracranial Injection of rAAV Vectors

R6/2 and wild-type mice at post-natal day ≈21 were anesthetized with somnopentyl (50 mg/kg body weight [b.w.]), and 2 μL of AAV9_miR-132 or AAV9_miR-Neg was stereotaxically injected into both sides of the striatum (≈1 mm anterior to bregma, ≈2 mm lateral to the midline, ≈3 mm ventral to the skull surface) using a Hamilton Neuros Syringe (HAMILTON, Reno, NV, USA).

Transfection

Transfection of plasmid DNAs into primary cultured cells was carried out by a Lipofectamine 2000 Reagent (Thermo Fisher Scientific) according to the manufacturer's instructions. Before transfection, culture medium was replaced with serum-free culture medium (Neurobasal medium supplemented with 2% B27 supplement, 1 mM glutamine, and 10 μM 2-mercaptoethanol) and incubated for 2 hr at 37°C in a 5% CO_2 humidified chamber. After incubation, plasmid DNA-Lipofectamine 2000 mixtures were added into the cells. Four hours after transfection, medium was replaced with fresh, complete culture medium containing FBS.

Rotarod Test

Rotarod test was carried out to see the motor coordination of mice, using an Ugo Basile Rota-Rod 47600 (Ugo Basile, Comerio, Italy). The apparatus was programmed to accelerate its rod rotation from 4 to 40 rpm during 300 s. Time from when mouse was put onto the

rod of the apparatus until when the mouse fell off or cling on to the rod was recorded. Mice were subjected to three trials per day between 2:00 and 7:00 p.m., and the test was performed for the third straight day.

Open Field Locomotors Activity and Rearing Frequency

Spontaneous locomotor activity and rearing frequency of mice were examined. Mice were placed in a monitoring box (40 cm × 28 cm × 31 cm) (SUPERMEX; Muromachi Kikai, Tokyo, Japan) equipped with an activity sensor (Pyroelectric sensor PYS-001; Muromachi Kikai) and a rearing sensor (MRS-110TX-RX; Muromachi Kikai) at the top and wall of the box, respectively. Locomotor activity and rearing frequency of a mouse in the box were simultaneously measured for 15 min, and the test was performed between 2:00 and 7:00 p.m. The obtained data were analyzed by a Data Collection Program CompACT AMS Ver.3 (Muromachi Kikai).

SDS-PAGE and Western Blotting

Cultured cells and brain samples were lysed in lysis buffer (20 mM Tris-HCl [pH 7.5], 150 mM NaCl, 1 mM EGTA, 1% Triton X-100) containing 1× protease inhibitor cocktail (Protease Inhibitor Cocktail Tablets; Roche). The lysate was homogenized with a pestle and centrifuged at 3,000 × *g* for 10 min at 4°C and then further centrifuged at 14,000 × *g* for 15 min at 4°C. The resultant supernatant was collected, and protein concentration was measured by a Protein Quantification kit (DOJINDO, Mashiki-town, Kumamoto, Japan) according to the manufacturer's instructions. Equal amounts of protein (≈40 μg) were mixed with 4× sample buffer (0.25 M Tris-HCl, 40% glycerol, 8% SDS, 0.04% bromophenol blue, 8% beta-mercaptoethanol), boiled for 5 min, and separated by SDS-PAGE with 10% polyacrylamide gels. After separation, proteins were electrophoretically blotted onto polyvinylidene fluoride membranes (Immobilon P; Millipore, Billerica, MA, USA). The membranes were blocked for 1 hr in blocking solution (5% BSA [Sigma-Aldrich] in TBS-T buffer [Tris-buffered saline (TBS) containing 0.1% Tween 20]) and incubated with diluted primary antibodies (indicated below) at 4°C overnight. After incubation, the membranes were washed in TBS-T buffer and incubated with 1/5,000 diluted horseradish peroxidase (HRP)-conjugated goat anti-mouse IgG (Sigma-Aldrich) or goat anti-rabbit IgG (Sigma-Aldrich), or with 1/500 diluted VerBlot for IP secondary antibody (HRP) (ab131366; Abcam) for 1 hr at room temperature. Antigen-antibody complexes were visualized using Immobilon Western Chemiluminescent HRP Substrate (Millipore). The primary antibodies used, as well as their dilution ratios including IDs and manufactures in parentheses, are as follows: anti-AGO2 (1:1,000; 2897; CST), anti-MeCP2 (1:1,000; 3456; CST), anti-Ptbp2 (1:1,000; ab154787; Abcam), anti-RFX4 (1:1,000; LS-C109967; LSBio, Seattle, WA, USA), anti-Gapdh (1:1,000; 2118; CST), anti-HTT (1/300; MAB5374; Millipore), anti-alpha-tubulin (1/10,000; F2168, Sigma-Aldrich), anti-MAP2 (1:1,000; ab32454; Abcam), anti-GFAP (1:1,000; G3893; Sigma-Aldrich), and anti-p250GAP antibodies (1:5,000) that were kindly provided by Dr. T. Nakazawa (Osaka University).[43,44] Anti-Ago2 (1:1,000, ab32381; Abcam) was used for detection of Ago2 in IP samples.

Fluorescence Immunocytochemistry and Immunohistochemistry

Cultured cells were rinsed with PBS, fixed with 4% paraformaldehyde (PFA) in PBS, permeabilized with 0.2% Triton-X in PBS for 5 min at room temperature and incubated in blocking solution (5% BSA [Sigma-Aldrich] and 5% goat serum [Cell Signaling Technology, Danvers, MA, USA]) for 1 hr at room temperature. The treated cells were incubated with diluted primary antibodies (indicated below) in PBS at 4°C overnight. After washed with PBS, antigen-antibody complexes were visualized by isotype-specific secondary antibodies conjugated with Alexa 488 or Alexa 594 (Molecular Probes, CA, USA). In addition, nuclear staining was also carried out with 2 μg/mL Hoechst33342 (Cell Signaling Technology) or 2 μg/mL propidium iodide (Thermo Fisher Scientific) in PBS. Stained cells were examined using a ZEISS fluorescent microscope (Axiovert 40 CFL).

For immunohistochemical analysis, dissected brain tissues were fixed with 4% PFA in PBS at 4°C overnight, incubated in 20% sucrose in PBS at 4°C overnight, embedded in O.C.T. compound (Sakura Finetech Japan, Koto-ku, Tokyo, Japan) on a dry ice/ethanol bath, and then cut into 15-μm-thick sections. Cryosections were treated in blocking/permeabilization buffer (0.3% Triton X-100 and 5% goat serum in PBS) for 30 min at room temperature and incubated with diluted primary antibodies (indicated below) in PBS containing 0.1% Triton X-100 and 5% goat serum at 4°C overnight. After washing with PBS, the sections were incubated with isotype-specific secondary antibodies conjugated with Alexa 488 or Alexa 594 (Molecular Probes), and examined using a Leica confocal fluorescent microscope (Leica TCS SP2). Nuclei were also stained with Hoechst33342 and examined. The primary antibodies used, as well as their dilution ratios including IDs and manufactures in parentheses, are as follows: anti-HTT (1/200, MAB5374; Millipore) and anti-GFP (1/500, A11122; Thermo Fisher Scientific).

Statistical Analysis

Data obtained in this study were initially evaluated by one-way ANOVA. If significant difference between data was detected by ANOVA, Tukey's post hoc test was carried out between the data of interest. The level of statistical significance was set at 0.05.

ACCESSION NUMBERS

The accession number of the miRNA expression data used in this study is GEO: GSE100792.

SUPPLEMENTAL INFORMATION

Supplemental Information includes seven figures and one table and can be found with this article online at https://doi.org/10.1016/j.omtn.2018.01.007.

AUTHOR CONTRIBUTIONS

H.H., M.F., and M.T. designed research; M.F., M.T., H. Fujita, T.C., H.A.P., S.W., and H.H. performed experiments; H. Furuva, M.M., K.W., T.O., Y.N., and H.H. contributed new reagents/analytic tools;

M.F., M.T., and H.H. analyzed data; M.F., M.T., and H.H wrote the paper.

CONFLICTS OF INTEREST

H.H. and M.T. have a pending patent regarding the results of this study.

ACKNOWLEDGMENTS

We would like to express our special thanks for the late Dr. Ichiro Kanazawa. We are sincerely grateful for his helpful advice, encouragement, and support to this work. We would like to thank Dr. T. Nakazawa for kindly providing anti-p250GAP antibodies. We also thank Dr. T. Kabuta and A. Eda for their helpful advice and assistance. This work was supported by the practical research project for rare/intractable diseases from Japan Agency for Medical Research and Development (grants 16ek0109008h0003 and 17ek0109190h0002); research grants from the Ministry of Health, Labour and Welfare, Japan; and Grants-in-Aid for Young Scientists (B) (grants 25871169 and 16K19003), Grants-in-Aid for Scientific Research (B) (grant 24390226), and Grant-in-Aid for Challenging Exploratory Research (grant 25670428) from the Japan Society for the Promotion of Science.

REFERENCES

1. Walker, F.O. (2007). Huntington's disease. Lancet *369*, 218–228.
2. Ross, C.A., Aylward, E.H., Wild, E.J., Langbehn, D.R., Long, J.D., Warner, J.H., Scahill, R.I., Leavitt, B.R., Stout, J.C., Paulsen, J.S., et al. (2014). Huntington disease: natural history, biomarkers and prospects for therapeutics. Nat. Rev. Neurol. *10*, 204–216.
3. Krol, J., Loedige, I., and Filipowicz, W. (2010). The widespread regulation of microRNA biogenesis, function and decay. Nat. Rev. Genet. *11*, 597–610.
4. Lagos-Quintana, M., Rauhut, R., Yalcin, A., Meyer, J., Lendeckel, W., and Tuschl, T. (2002). Identification of tissue-specific microRNAs from mouse. Curr. Biol. *12*, 735–739.
5. Liu, C.G., Calin, G.A., Meloon, B., Gamliel, N., Sevignani, C., Ferracin, M., Dumitru, C.D., Shimizu, M., Zupo, S., Dono, M., et al. (2004). An oligonucleotide microchip for genome-wide microRNA profiling in human and mouse tissues. Proc. Natl. Acad. Sci. USA *101*, 9740–9744.
6. Babak, T., Zhang, W., Morris, Q., Blencowe, B.J., and Hughes, T.R. (2004). Probing microRNAs with microarrays: tissue specificity and functional inference. RNA *10*, 1813–1819.
7. Hohjoh, H., and Fukushima, T. (2007). Marked change in microRNA expression during neuronal differentiation of human teratocarcinoma NTera2D1 and mouse embryonal carcinoma P19 cells. Biochem. Biophys. Res. Commun. *362*, 360–367.
8. Hohjoh, H., and Fukushima, T. (2007). Expression profile analysis of microRNA (miRNA) in mouse central nervous system using a new miRNA detection system that examines hybridization signals at every step of washing. Gene *391*, 39–44.
9. Lu, M., Zhang, Q., Deng, M., Miao, J., Guo, Y., Gao, W., and Cui, Q. (2008). An analysis of human microRNA and disease associations. PLoS ONE *3*, e3420.
10. Jackson, A.L., and Levin, A.A. (2012). Developing microRNA therapeutics: approaching the unique complexities. Nucleic Acid Ther. *22*, 213–225.
11. Soifer, H.S., Rossi, J.J., and Saetrom, P. (2007). MicroRNAs in disease and potential therapeutic applications. Mol Ther. *15*, 2070–2079.
12. Eda, A., Takahashi, M., Fukushima, T., and Hohjoh, H. (2011). Alteration of microRNA expression in the process of mouse brain growth. Gene *485*, 46–52.
13. Wanet, A., Tacheny, A., Arnould, T., and Renard, P. (2012). miR-212/132 expression and functions: within and beyond the neuronal compartment. Nucleic Acids Res. *40*, 4742–4753.
14. Magill, S.T., Cambronne, X.A., Luikart, B.W., Lioy, D.T., Leighton, B.H., Westbrook, G.L., Mandel, G., and Goodman, R.H. (2010). microRNA-132 regulates dendritic growth and arborization of newborn neurons in the adult hippocampus. Proc. Natl. Acad. Sci. USA *107*, 20382–20387.
15. Remenyi, J., van den Bosch, M.W., Palygin, O., Mistry, R.B., McKenzie, C., Macdonald, A., Hutvagner, G., Arthur, J.S., Frenguelli, B.G., and Pankratov, Y. (2013). miR-132/212 knockout mice reveal roles for these miRNAs in regulating cortical synaptic transmission and plasticity. PLoS ONE *8*, e62509.
16. Remenyi, J., Hunter, C.J., Cole, C., Ando, H., Impey, S., Monk, C.E., Martin, K.J., Barton, G.J., Hutvagner, G., and Arthur, J.S. (2010). Regulation of the miR-212/132 locus by MSK1 and CREB in response to neurotrophins. Biochem. J. *428*, 281–291.
17. Lee, S.T., Chu, K., Im, W.S., Yoon, H.J., Im, J.Y., Park, J.E., Park, K.H., Jung, K.H., Lee, S.K., Kim, M., and Roh, J.K. (2011). Altered microRNA regulation in Huntington's disease models. Exp. Neurol. *227*, 172–179.
18. Johnson, R., Zuccato, C., Belyaev, N.D., Guest, D.J., Cattaneo, E., and Buckley, N.J. (2008). A microRNA-based gene dysregulation pathway in Huntington's disease. Neurobiol. Dis. *29*, 438–445.
19. Klein, M.E., Lioy, D.T., Ma, L., Impey, S., Mandel, G., and Goodman, R.H. (2007). Homeostatic regulation of MeCP2 expression by a CREB-induced microRNA. Nat. Neurosci. *10*, 1513–1514.
20. Impey, S., Davare, M., Lesiak, A., Fortin, D., Ando, H., Varlamova, O., Obrietan, K., Soderling, T.R., Goodman, R.H., and Wayman, G.A. (2010). An activity-induced microRNA controls dendritic spine formation by regulating Rac1-PAK signaling. Mol. Cell. Neurosci. *43*, 146–156.
21. Vo, N., Klein, M.E., Varlamova, O., Keller, D.M., Yamamoto, T., Goodman, R.H., and Impey, S. (2005). A cAMP-response element binding protein-induced microRNA regulates neuronal morphogenesis. Proc. Natl. Acad. Sci. USA *102*, 16426–16431.
22. Wayman, G.A., Davare, M., Ando, H., Fortin, D., Varlamova, O., Cheng, H.Y., Marks, D., Obrietan, K., Soderling, T.R., Goodman, R.H., and Impey, S. (2008). An activity-regulated microRNA controls dendritic plasticity by down-regulating p250GAP. Proc. Natl. Acad. Sci. USA *105*, 9093–9098.
23. Smith, P.Y., Delay, C., Girard, J., Papon, M.A., Planel, E., Sergeant, N., Buée, L., and Hébert, S.S. (2011). MicroRNA-132 loss is associated with tau exon 10 inclusion in progressive supranuclear palsy. Hum. Mol. Genet. *20*, 4016–4024.
24. Cheng, H.Y., Papp, J.W., Varlamova, O., Dziema, H., Russell, B., Curfman, J.P., Nakazawa, T., Shimizu, K., Okamura, H., Impey, S., and Obrietan, K. (2007). microRNA modulation of circadian-clock period and entrainment. Neuron *54*, 813–829.
25. Mazziotti, R., Baroncelli, L., Ceglia, N., Chelini, G., Sala, G.D., Magnan, C., Napoli, D., Putignano, E., Silingardi, D., Tola, J., et al. (2017). Mir-132/212 is required for maturation of binocular matching of orientation preference and depth perception. Nat. Commun. *8*, 15488.
26. Mangiarini, L., Sathasivam, K., Seller, M., Cozens, B., Harper, A., Hetherington, C., Lawton, M., Trottier, Y., Lehrach, H., Davies, S.W., and Bates, G.P. (1996). Exon 1 of the HD gene with an expanded CAG repeat is sufficient to cause a progressive neurological phenotype in transgenic mice. Cell *87*, 493–506.
27. Carter, R.J., Lione, L.A., Humby, T., Mangiarini, L., Mahal, A., Bates, G.P., Dunnett, S.B., and Morton, A.J. (1999). Characterization of progressive motor deficits in mice transgenic for the human Huntington's disease mutation. J. Neurosci. *19*, 3248–3257.
28. Michalik, A., and Van Broeckhoven, C. (2003). Pathogenesis of polyglutamine disorders: aggregation revisited. Hum. Mol. Genet. *12*, R173–R186.
29. Takahashi, M., Watanabe, S., Murata, M., Furuya, H., Kanazawa, I., Wada, K., and Hohjoh, H. (2010). Tailor-made RNAi knockdown against triplet repeat disease-causing alleles. Proc. Natl. Acad. Sci. USA *107*, 21731–21736.
30. Lombardi, M.S., Jaspers, L., Spronkmans, C., Gellera, C., Taroni, F., Di Maria, E., Donato, S.D., and Kaemmerer, W.F. (2009). A majority of Huntington's disease patients may be treatable by individualized allele-specific RNA interference. Exp. Neurol. *217*, 312–319.
31. Pfister, E.L., Kennington, L., Straubhaar, J., Wagh, S., Liu, W., DiFiglia, M., Landwehrmeyer, B., Vonsattel, J.P., Zamore, P.D., and Aronin, N. (2009). Five siRNAs targeting three SNPs may provide therapy for three-quarters of Huntington's disease patients. Curr. Biol. *19*, 774–778.

32. Hohjoh, H. (2013). Disease-causing allele-specific silencing by RNA interference. Pharmaceuticals (Basel) *6*, 522–535.

33. Benraiss, A., Wang, S., Herrlinger, S., Li, X., Chandler-Militello, D., Mauceri, J., Burm, H.B., Toner, M., Osipovitch, M., Jim Xu, Q., et al. (2016). Human glia can both induce and rescue aspects of disease phenotype in Huntington disease. Nat. Commun. *7*, 11758.

34. Chen, R., Shi, L., Hakenberg, J., Naughton, B., Sklar, P., Zhang, J., Zhou, H., Tian, L., Prakash, O., Lemire, M., et al. (2016). Analysis of 589,306 genomes identifies individuals resilient to severe Mendelian childhood diseases. Nat. Biotechnol. *34*, 531–538.

35. Hébert, S.S., Wang, W.X., Zhu, Q., and Nelson, P.T. (2013). A study of small RNAs from cerebral neocortex of pathology-verified Alzheimer's disease, dementia with lewy bodies, hippocampal sclerosis, frontotemporal lobar dementia, and non-demented human controls. J. Alzheimers Dis. *35*, 335–348.

36. Lau, P., Bossers, K., Janky, R., Salta, E., Frigerio, C.S., Barbash, S., Rothman, R., Sierksma, A.S., Thathiah, A., Greenberg, D., et al. (2013). Alteration of the microRNA network during the progression of Alzheimer's disease. EMBO Mol. Med. *5*, 1613–1634.

37. Wong, H.K., Veremeyko, T., Patel, N., Lemere, C.A., Walsh, D.M., Esau, C., Vanderburg, C., and Krichevsky, A.M. (2013). De-repression of FOXO3a death axis by microRNA-132 and -212 causes neuronal apoptosis in Alzheimer's disease. Hum. Mol. Genet. *22*, 3077–3092.

38. Miller, B.H., Zeier, Z., Xi, L., Lanz, T.A., Deng, S., Strathmann, J., Willoughby, D., Kenny, P.J., Elsworth, J.D., Lawrence, M.S., et al. (2012). MicroRNA-132 dysregulation in schizophrenia has implications for both neurodevelopment and adult brain function. Proc. Natl. Acad. Sci. USA *109*, 3125–3130.

39. McFarland, K.N., Huizenga, M.N., Darnell, S.B., Sangrey, G.R., Berezovska, O., Cha, J.H., Outeiro, T.F., and Sadri-Vakili, G. (2014). MeCP2: a novel Huntingtin interactor. Hum. Mol. Genet. *23*, 1036–1044.

40. Popiel, H.A., Takeuchi, T., Fujita, H., Yamamoto, K., Ito, C., Yamane, H., Muramatsu, S., Toda, T., Wada, K., and Nagai, Y. (2012). Hsp40 gene therapy exerts therapeutic effects on polyglutamine disease mice via a non-cell autonomous mechanism. PLoS ONE *7*, e51069.

41. Okada, T., Nonaka-Sarukawa, M., Uchibori, R., Kinoshita, K., Hayashita-Kinoh, H., Nitahara-Kasahara, Y., Takeda, S., and Ozawa, K. (2009). Scalable purification of adeno-associated virus serotype 1 (AAV1) and AAV8 vectors, using dual ion-exchange adsorptive membranes. Hum. Gene Ther. *20*, 1013–1021.

42. Liu, W.Z., Goto, J., Wang, Y.L., Murata, M., Wada, K., and Kanazawa, I. (2003). Specific inhibition of Huntington's disease gene expression by siRNAs in cultured cells. P Jpn Acad B-Phys. *79B*, 293–298.

43. Nakazawa, T., Watabe, A.M., Tezuka, T., Yoshida, Y., Yokoyama, K., Umemori, H., Inoue, A., Okabe, S., Manabe, T., and Yamamoto, T. (2003). p250GAP, a novel brain-enriched GTPase-activating protein for Rho family GTPases, is involved in the N-methyl-d-aspartate receptor signaling. Mol. Biol. Cell *14*, 2921–2934.

44. Nakazawa, T., Kuriu, T., Tezuka, T., Umemori, H., Okabe, S., and Yamamoto, T. (2008). Regulation of dendritic spine morphology by an NMDA receptor-associated Rho GTPase-activating protein, p250GAP. J. Neurochem. *105*, 1384–1393.